Journal of Alloys and Compounds 845 (2020) 155499

Contents lists available at ScienceDirect

Journal of Alloys and Compounds

journal homepage: http://www.elsevier.com/locate/jalcom

Structural, elastic, electronic, and magnetic properties of Si-doped Co_2MnGe full-Heusler type compounds

M. Özduran [a], A. Candan [b, *], S. Akbudak [c], A.K. Kushwaha [d], A. İyigör [b]

[a] Department of Physics, Faculty of Arts and Sciences, Ahi Evran University, 40100, Kırşehir, Turkey
[b] Department of Machinery and Metal Technology, Kırşehir Ahi Evran University, 40100, Kırşehir, Turkey
[c] Department of Physics, Faculty of Arts and Sciences, Adiyaman University, 02100, Adiyaman, Turkey
[d] Department of Physics, K.N. Govt. P.G. College, Gyanpur, Bhadohi, 221304, India

ARTICLE INFO

Article history:
Received 14 November 2019
Received in revised form
25 April 2020
Accepted 4 May 2020
Available online 11 May 2020

Keywords:
Half-metallicity
Density functional theory
Heusler compounds
Elastic constants

ABSTRACT

The structural, electronic, magnetic and elastic properties of $Co_2MnGe_{1-x}Si_x$ ($x = 0$, 0.25, 0.50, 0.75, and 1) compounds are investigated by first-principles calculations within the generalized gradient approximation (GGA). The calculated structural parameters of these compounds show a slightly decreasing lattice constants and similarly decreasing lattice volumes and enthalpies of formation on increasing Si substitution x. The band structure calculations estimate that these compounds at their optimized lattice constants are half-metallic ferromagnets. The calculated total magnetic moment values are all integers, which is typical for half-metallic materials with a half-metallic bandgap (E_{HM}) in the minority states. Besides, the total magnetic moments of these compounds are fully compatible with the Slater-Pauling rule showing the half-metallicity and large spin polarization desired for spintronics applications. The partial substitution of the Ge atom by the Si does not affect the atomic magnetic moment and total magnetic moment. The obtained values of structural parameters, total and atomic magnetic moments for $x = 0$ and 1 stoichiometric compounds are in good agreement with experimental and theoretical results. The elastic constants are studied for all compositions of x in order to verify the mechanical stability of these compounds. Born's stability criterion implemented on elastic constants of $Co_2MnGe_{1-x}Si_x$ ($x = 0$, 0.25, 0.50, 0.75, and 1) compounds confirm that these materials are mechanically stable. Other elastic parameters like bulk modulus (B), shear modulus (G), ratio of B/G, Young's modulus (E), Poisson's ratio (ν), and Shear anisotropic factor (A), which are the significant elastic moduli for technological applications have been thoroughly investigated. Consequently, these compounds, especially $Co_2MnGe_{1-x}Si_x$ ($x = 0.25$, 0.50, 0.75) mixed systems, are promising candidates for practical applications in the field of spin electronics.

1. Introduction

Thenceforward their reconnaissance in 1903 [1], Heusler alloys have attracted the attention of many researchers due to the fact that they are ideal materials for magneto-electronic applications and also show semi-conductive properties [2,3]. Apart from magneto-electronic applications, Heusler alloys show attractive properties for spintronics [4,5], optoelectronics [6,7], superconductivity [8], shape-memory [9] and thermoelectric [10] applications as well. Heusler alloys are divided into two parts as semi-Heusler alloys and full Heusler alloys and are represented by XYZ, X_2YZ stoichiometry, respectively. Here, X and Y are transition elements and Z is a p-block element (Z: Ga, Sb, Sn, In) in the periodic table. Semi and full Heusler alloys crystallize in $C1_b$ and $L2_1$, respectively. In the unit cell of full Heusler alloys, X atoms are situated in (0, 0, 0) and (1/2, 1/2, 1/2), Y atom in (1/4, 1/4, 1/4) and Z atom in (3/4, 3/4, 3/4) positions. With the discovery of large magnetoresistances (GMR) by Baibich et al. [11] and Binasch et al. [12] simultaneously, the main idea of magneto-electronics was formed. This idea continued with the proliferation of the devices that process the spin of the electron instead of the traditional devices using only the charge of the electron. Thus, the main motivation is to utilize the degree of freedom of electron spin in order to obtain better nano-electronic devices. Because it has been observed that adding the degree of freedom of spin to traditional electronic

* Corresponding author.
E-mail address: acandan@ahievran.edu.tr (A. Candan).

https://doi.org/10.1016/j.jallcom.2020.155499
0925-8388/

devices have significant advantages such as, increasing data processing speed, reducing electrical power usage and non-volatile memory. In 1983, De Groot et al. found that NiMnSb, an inter-metallic Heusler alloy, exhibited semi-metallic properties [13]. Then a few semi-metallic ferromagnetic materials and their properties were investigated theoretically with ab-initio calculations and later proved to be precise with the help of various experiments.

Initially, among semi-metallic materials, inter-metallic Heusler alloys have been the focus of interest due to their simple magnification and high Curie temperatures [14,15], but in recent years this interest has shifted to compounds described as full Heusler alloys and containing mainly Co and Mn such as Co_2MnSi and Co_2MnGe [16–30]. Studies given in Refs. [16–30] include experimental, theoretical and a combination of both experimental and theoretical works. To mention some of these studies; from an experimental perspective, Webster et al. [16] studied the saturation, magnetization X-ray and neutron diffraction of Co_2MnZ where Z = Al, Si, Ga, Fe, Sn, and Sb. This was the first study in which Webster has precisely determined each magnetic moment of atoms other than Mn. Using the vertical gradient freeze (VGF) technique in argon at atmospheric pressure, Manea and co-workers [17] analyzed the polycrystalline $Co_2Mn(Si, Ge, Ga, Sn, Sb_{0.8}Sn_{0.2})$ as targets for pulsed laser deposition of magnetic contacts for spintronic devices. Kandpal et al. [22] studied the bandgap, transport properties and magnetic behavior of A_2BC Heusler compounds utilizing first-principles density functional theory (DFT) calculations within LDA + U. However, since theory goes hand in hand with experiments, ab initio calculations which pave the way for better material design due to their good match with experimental results dominates the theoretical studies conducted about Co and Mn-based full Heusler alloys. To touch on some of these theoretical studies, Picozzi and co-workers [23] investigated the structural, electronic, and magnetic properties of Co_2MnX (X = Si, Ge, Sn) at zero and elevated pressure values using DFT calculations within local spin density approximation (LSDA) and generalized gradient approximation (GGA). Wu et al. [24] studied the elastic properties of cubic Co_2YZ compounds with $L2_1$ structure through first-principles density functional theory calculations within the full-potential linearized augmented plane wave (FLAPW) technique. Rai et al. [25] performed first-principles DFT calculation based on GGA and LSDA to observe the electronic and magnetic properties of Co_2MnGe and Co_2MnSn. In some other studies, it has been observed that energy gaps and structural parameters change significantly by partial substitution of X and Y atoms in Co_2XYZ alloys [31–34]. The use of Heusler alloys, especially in spintronic and electronic applications is because they have appropriate and tunable bandgap values. This tunable bandgap characteristic enables us to make devices with suitable band gap values to be used in future electronics and spintronic applications. One of the suitable methods to tune the bandgap value of Heusler alloys is doping the alloy with concordant atoms. Despite the large number of studies about Co_2MnX (X = Si, Ge), which were mentioned above, studies including the partial substitution of Si and Ge atoms are very limited. To fill this gap and search the potential applicability of Co_2MnX (X = Si, Ge) in spintronic and electronic applications, we have performed first-principles calculations within the GGA method to investigate the structural, elastic, half-metallic and electronic properties of $Co_2MnGe_{1-x}Si_x$ (x = 0, 0.25, 0.50, 0.75, and 1) compounds.

2. Computational details

All calculations were performed by using the Vienna Ab initio Simulation Package (VASP) [35,36], which exploits plane-wave basis sets and periodic boundary conditions. Energies of core electrons were modeled using projector augmented-wave (PAW) [37,38] pseudopotentials to cut-off energy of 500 eV, exchange and correlation of valence electrons were modeled using the Perdew-Burke-Ernzerhof (PBE) [39] functional. Methfessel-Paxton with a smearing factor of 0.225 eV was used to set the partial occupancies of each orbital [40]. The structural optimizations were implemented for all structures and the k-point meshes were selected Γ-centered 12 × 12 × 12 Monkhorst-Pack scheme [41] for cubic phases (*Fm-3m* and *Pm-3m*) and 10 × 10 × 7 for tetragonal phase (*P4-mmm*). Electronic structures were converged self-consistently until the difference in energy between subsequent iterations was not larger than 10^{-5} eV. The stress-strain relationship [42] was used for the calculation of elastic properties.

3. Result and discussions

3.1. Structural properties

The full-Heusler X_2YZ compounds crystallize with Cu_2MnAl and Hg_2CuTi crystal structures. These structures have four interpenetrating fcc sublattices. In the case of Cu_2MnAl-type crystal structure, the X atoms occupy the (0, 0, 0) and (1/2, 1/2, 1/2) positions, Y atom occupies the (1/4, 1/4, 1/4) position and the Z atom occupies (3/4, 3/4, 3/4) position [43]. On the other hand, for the case of Hg_2CuTi-type crystal structure, the X atoms occupy the positions (0, 0, 0) and (1/4, 1/4, 1/4), Y atom occupies the position (1/2, 1/2, 1/2) and the Z atom occupies the position (3/4, 3/4, 3/4) [44,45].

Co-based Heusler compounds Co_2MnX (M = Si, Ge, etc.) have been extensively studied by many researchers. The obtained crystallographic data in different studies, which was experimentally performed with the X-ray diffraction method, reveals the fact that the pure phase is the $L2_1$ structure with the space group Fm-3m (Cu_2MnAl-type crystal structure) for the Co_2MnSi single crystal [16,46,47]. In addition, two theoretically conducted studies [48,49], which used total energy calculations for Co_2MnGe and Co_2MnSi compounds, showed that the formation of these alloys in Cu_2MnAl-type structure is energetically favorable. Besides, they found that the Cu_2MnAl-type structure is more stable than the Hg_2CuTi-type structure for the ferromagnetic state. Therefore, the structural optimization of the pure Co_2MnGe and Co_2MnSi Heusler compounds has been investigated in the Cu_2MnAl type crystal structure.

It has been established that the pure system Co_2MnGe and Co_2MnSi have a face-centered cubic structure with space group *Fm-3m* (225) while the mixed compounds at compositions 0.25 and 0.75 have a primitive cubic structure with space group *Pm-3m* (221). At composition 0.50, i.e., $Co_2MnGe_{0.50}Si_{0.50}$ mixed compound has a tetragonal *P4/mmm* structure. The number of atoms are listed in the unit cell of the mixed compounds at various compositions in Table 2. Besides, Fig. 1(a–e) shows the crystal structure of Co_2MnGe, Co_2MnSi, $Co_2MnGe_{0.75}Si_{0.25}$, $Co_2MnGe_{0.25}Si_{0.75}$ and $Co_2MnGe_{0.5}Si_{0.5}$, respectively.

The comparison between our calculated structural parameters for Co_2MnX (X = Si, Ge) and experimental and theoretical results are presented in Table 1. The obtained structural parameters indicate that the lattice constant (a_0) and volume (V_0) of these compounds slightly decrease with growing Si constituent. Additionally, the calculated equilibrium lattice constant (a_0) and enthalpies of formation (ΔH_f) for Co_2MnSi and Co_2MnGe are consistent with experimental [16,17,22,30] and theoretical studies [18,20,21,23–28]. To the best of our knowledge, there is no study to compare the results of x = 0.25, 0.50, 0.75 mixed systems. Therefore, the following Vegard's Law [50] is used to estimate their lattice constants.

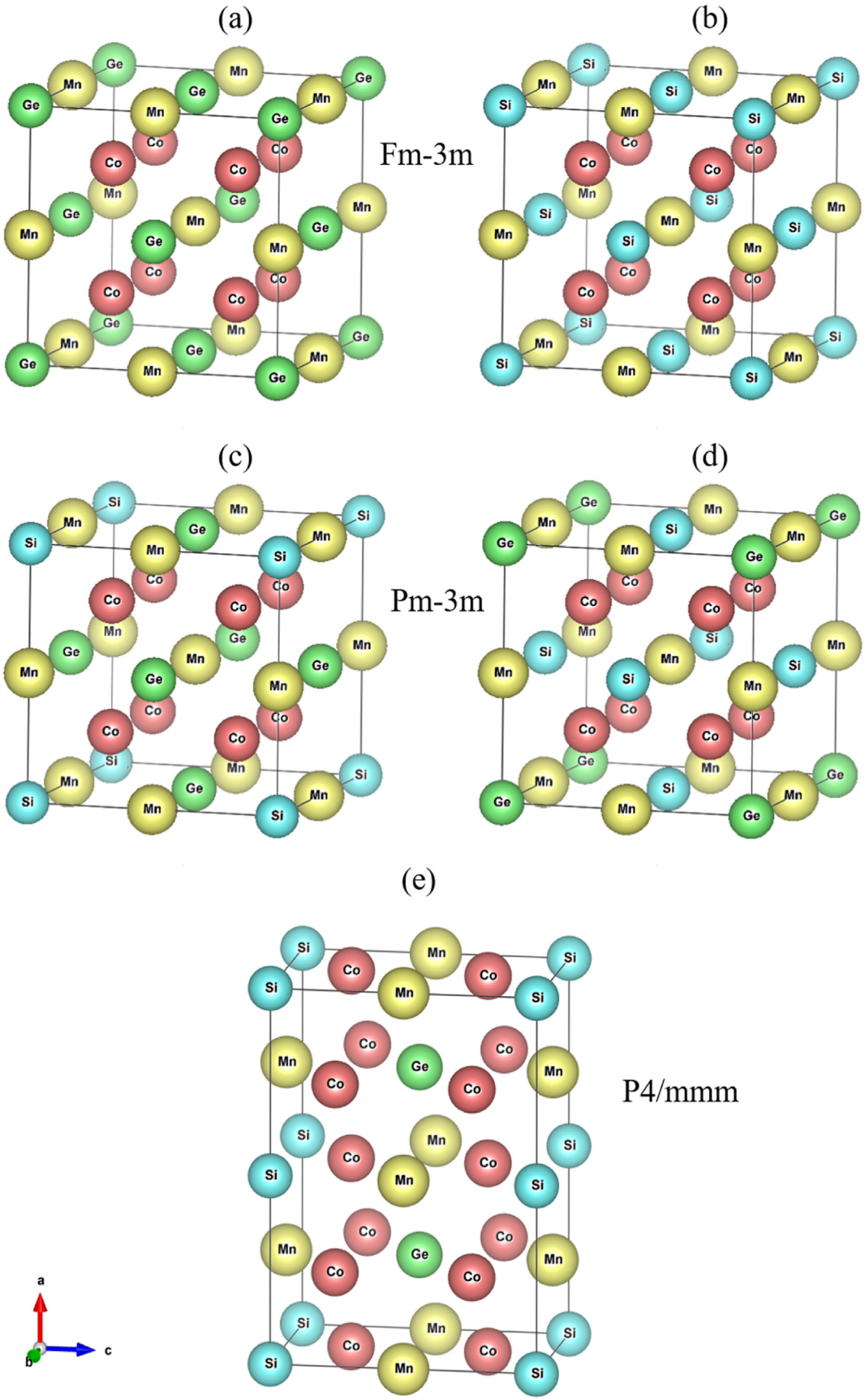

Fig. 1. The crystal structure of (a) Co_2MnGe (b) Co_2MnSi (c) $Co_2MnGe_{0.75}Si_{0.25}$ (d) $Co_2MnGe_{0.25}Si_{0.75}$ and (e) $Co_2MnGe_{0.5}Si_{0.5}$ compounds.

Table 1
The calculated lattice parameters of $Co_2MnGe_{1-x}Si_x$ ($x = 0$, 0.25, 0.50, 0.75, and 1) compounds.

Composition	Space group	Ref.	a_0 (Å)	V_0 (Å^3)	ΔH_f (eV/atom)
Co_2MnGe	*Fm-3m* (225)	Present	5.727	187.841	−0.361
		[16]$^{Exp.}$	5.743	–	–
		[17]$^{Exp.}$	5.753	–	–
		[22]$^{Exp.}$	5.749	–	–
		[30]$^{Exp.}$	5.746	–	−0.328
		[18]	5.753	–	–
		[20]	5.770	–	–
		[21]	5.711	–	–
		[23]^{GGA}	5.734	–	–
		[23]^{LSDA}	5.613	–	–
		[24]	5.730	–	−0.344
		[25]^{LSDA}	5.678	–	–
$Co_2MnGe_{0.75}Si_{0.25}$	*Pm-3m* (221)	Present	5.701	185.304	−0.409
$Co_2MnGe_{0.5}Si_{0.5}$	*P4/mmm* (123)	Present	a = 5.689 c = 4.012	183.091	−0.458
$Co_2MnGe_{0.25}Si_{0.75}$	*Pm-3m* (221)	Present	5.648	180.165	−0.507
Co_2MnSi	*Fm-3m* (225)	Present	5.622	177.701	−0.558
		[16]$^{Exp.}$	5.654	–	–
		[17]$^{Exp.}$	5.673	–	–
		[22]$^{Exp.}$	5.645	–	–
		[30]$^{Exp.}$	5.645	–	−0.439
		[18]	5.633	–	–
		[21]	5.606	–	–
		[23]^{GGA}	5.634	–	–
		[23]^{LSDA}	5.512	–	–
		[24]	5.643	–	−0.532
		[26]	5.627	–	−0.45
		[27]	5.582	–	–
		[28]	5.646	–	−0.465

Table 2
The compositions of each atom in $Co_2MnGe_{1-x}Si_x$ ($x = 0$, 0.25, 0.50, 0.75, and 1) compounds with the supercell method.

$Co_2MnGe_{1-x}Si_x$	Co	Mn	Ge	Si	Total
$x = 0.00$	8	4	4	–	16
$x = 0.25$	8	4	3	1	16
$x = 0.50$	8	4	2	2	16
$x = 0.75$	8	4	1	3	16
$x = 1.00$	8	4	4	–	16

$$a_0\ (Co_2MnGe_{0.75}Si_{0.25}) = 5.727 \times 0.75 + 5.622 \times 0.25 = 5.701\ \text{Å}$$

$$a_0\ (Co_2MnGe_{0.5}Si_{0.5}) = 5.727 \times 0.5 + 5.622 \times 0.5 = 5.675\ \text{Å}$$

$$a_0\ (Co_2MnGe_{0.25}Si_{0.75}) = 5.727 \times 0.25 + 5.622 \times 0.75 = 5.648\ \text{Å} \quad (1)$$

The Perdew–Burke–Ernzerhof (PBE) [39] GGA is one of the most widely used functional in Density Functional calculations. However, it is known that GGA-PBE slightly overestimates the lattice parameters at low temperatures. For Co_2MnGe and Co_2MnSi, the amount of deviation from both theoretical [18,20,21,23–26] and experimental [16,17,22,30] values is less than 1%. Therefore, the close compromise between the lattice parameters supports the credibility and robustness of our calculation method.

We have also computed the enthalpies of formation (ΔH_f) per atom for these compounds and collected the results in Table 1. As seen in Table 1, The negative enthalpies of formation indicate that these materials are thermodynamically stable in the studied structures. It can be concluded that the stability of these compounds decreases in the sequence of Co_2MnSi > $Co_2MnGe_{0.25}Si_{0.75}$ > $Co_2MnGe_{0.5}Si_{0.5}$ > $Co_2MnGe_{0.75}Si_{0.25}$ > Co_2MnGe. Namely, as the silicon concentration increases, the related structures of the compounds become more thermodynamically stable.

3.2. Elastic and related properties

Elastic properties contain important information about the structural stability, hardness, type of bonding between atoms and anisotropy of solid materials. The elastic properties of $Co_2MnGe_{1-x}Si_x$ for $x = 0$, 0.25, 0.50, 0.75, and 1 have been computed using the stress-strain method. It is known that the studied compounds are cubic at $x = 0$ and 1 with space group *Fm-3m* (225) and at $x = 0.25$ and 0.75 with space group *Pm-3m* (221) and lastly at $x = 0.50$ it contains a tetragonal structure with space group *P4/mmm* (123). Therefore, it is inferred that three elastic constants C_{11}, C_{12}, and C_{44} are required to understand the elastic properties of the studied compounds at compositions $x = 0$, 0.25, 0.75, and 1, but six elastic constants, i.e., C_{11}, C_{12}, C_{13}, C_{33}, C_{44}, and C_{66} are required to understand the elastic nature of the studied compound at composition $x = 0.50$. The calculated elastic constants for all x compositions are summarized in Table 3 with the available results in the literature [18,20,24,27,28]. It is well known that the Born's stability criterion for cubic structure is [27],

$$(C_{11} - C_{12}) > 0;\ C_{12} < B < C_{11};\ (C_{11} + 2C_{12}) > 0;\ C_{44} > 0 \quad (2)$$

and the Born's stability criterion for tetragonal structure is [51],

$$C_{11} > 0;\ C_{33} > 0;\ C_{44} > 0;\ C_{66} > 0;\ (C_{11} - C_{12}) > 0;\ (C_{11} + C_{33} - 2C_{13}) > 0,$$

$$(2C_{11} + C_{33} + 2C_{12} + 4C_{13}) > 0 \quad (3)$$

From Table 3, it is observed that the studied compounds are mechanically stable at all compositions of x, because of the fact that

Table 3
The calculated elastic constants C_{ij} (GPa) of $Co_2MnGe_{1-x}Si_x$ ($x = 0$, 0.25, 0.50, 0.75, and 1) compounds for various compositions.

Composition	Ref.	C_{11} (GPa)	C_{12} (GPa)	C_{44} (GPa)	C_{33} (GPa)	C_{13} (GPa)	C_{66} (GPa)
Co_2MnGe	Present	269.18	147.16	131.02	–	–	–
	[18]	270.53	153.77	126.55	–	–	–
	[20]	289	144	140	–	–	–
	[24]	272.8	160.0	137.9	–	–	–
$Co_2MnGe_{0.75}Si_{0.25}$	Present	281.60	150.01	134.99	–	–	–
$Co_2MnGe_{0.5}Si_{0.5}$	Present	358.33	87.82	68.08	313.75	165.51	136.95
$Co_2MnGe_{0.25}Si_{0.75}$	Present	305.63	153.71	141.63	–	–	–
Co_2MnSi	Present	314.23	174.42	143.10	–	–	–
	[18]	311.16	164.75	153.26	–	–	–
	[24]	310.5	174.2	156.9	–	–	–
	[27]	313.91	203.44	101.58	–	–	–
	[28]	316	174	143	–	–	–

they satisfy Born's stability criterion. From the results that belong to the calculated elastic constants, we can make the following conclusions;

I. The studied compounds are in the cubic structure at compositions $x = 0$, 0.25, 0.75, and 1. Elastic constant C_{11} represents the linear compression along a-axis of compounds having the cubic structure [52,53]. The other two elastic constants C_{12} and C_{44} show little resistance to surface and shear deformation, respectively. It is observed that C_{11} is more susceptible to the variation of Si composition compared to the C_{12} and C_{44}. It can also be concluded from Table 3 that the compressibility of these compounds decreases as $Co_2MnGe > Co_2MnGe_{0.75}Si_{0.25} > Co_2MnGe_{0.25}Si_{0.75} > Co_2MnSi$. Besides, as the Si content rises, the elastic constants (C_{11}, C_{12}, and C_{44}) of the $x = 0$, 0.25, 0.75, and 1 increase.

For $x = 0.5$, the stiffness against compressional strains is represented by the elastic constants C_{11} and C_{33} along the directions [100] and [001] and shear deformation is represented by the elastic constants C_{44} and C_{66}. Table 3 shows that C_{11} is larger than C_{33} which means that the studied crystal has more stiffness along [100] direction in comparison to the [001] direction. Besides, Table 3 also shows that C_{11} and C_{33} are larger than C_{44} and C_{66}, which also means that the examined material has more stiffness against strains along principal directions [100] and [001] that the shear deformation.

II. Making a large single crystal of any compound is challenging and hence it is very difficult to measure the elastic constants of the materials experimentally. The bulk modulus and shear modulus give the knowledge about the resistance against the change in volume due to external hydrostatic pressure and resistance against reversible deformations. Therefore, we have calculated the bulk modulus B and shear modulus G by using Voigt-Reuss-Hill approximations [54–56]. The Voigt (V) and Reuss (R) approximations of bulk modulus B (B_R and B_V) and shear modulus G (G_R and G_V) for cubic structure, i.e. for the composition $x = 0$, 0.25, 0.75 and 1:

$$B = B_V = B_R = \frac{1}{3}(C_{11} + 2C_{12}) \tag{4}$$

$$G_V = \frac{1}{5}(C_{11} - C_{12} + 3C_{44}) \tag{5}$$

$$G_R = \frac{5C_{44}(C_{11} - C_{12})}{4C_{44} + 3(C_{11} - C_{12})} \tag{6}$$

$$G = \frac{1}{2}(G_V + G_R) \tag{7}$$

and for tetragonal structure, i.e., for the composition $x = 0.50$:

$$B_V = \frac{1}{9}(2C_{11} + 2C_{12} + C_{33} + 4C_{13}) \tag{8}$$

$$B_R = \frac{C^2}{M} \tag{9}$$

$$G_V = \frac{1}{30}(M + 3C_{11} - 3C_{12} + 12C_{44} + 6C_{66}) \tag{10}$$

$$G_R = 15\left\{\frac{18B_V}{C^2} + \frac{6}{C_{11} - C_{12}} + \frac{6}{C_{44}} + \frac{3}{C_{66}}\right\}^{-1} \tag{11}$$

$$M = C_{11} + C_{12} + 2C_{33} - 4C_{13} \tag{12}$$

$$C^2 = (C_{11} + C_{12})C_{33} - C_{13}^2 \tag{13}$$

The calculated bulk modulus B and shear modulus G are collected in Table 4. It is observed from Table 4 that the bulk modulus of the studied compounds increases with growing Si constituent for cubic structure, i.e. for the composition of $x = 0$, 0.25, 0.75, and 1. Besides, we can say that the resistance against volume change due to hydrostatic pressure follows the sequence that is $Co_2MnGe < Co_2MnGe_{0.75}Si_{0.25} < Co_2MnGe_{0.25}Si_{0.75} < Co_2MnGe_{0.50}Si_{0.50} < Co_2MnSi$.

III. The Young's modulus (E) of any material represents the resistance against uniaxial tension because of the stiffness of the materials. The Young's modulus of the studied materials for all x compositions have been calculated using obtained B and G with the help of the relation:

$$E = \frac{9BG}{(3B + G)} \tag{14}$$

The calculated Young's modulus E for these compounds are given in Table 4. It is concluded that the Young's modulus of the studied materials decreases in the sequence of $Co_2MnGe_{0.25}Si_{0.75} > Co_2MnSi > Co_2MnGe_{0.75}Si_{0.25} > Co_2MnGe > Co_2MnGe_{0.50}Si_{0.50}$. Besides, the Vickers hardness of these compounds has computed with the help of the following equation [57] and results are given in Table 4.

$$H_V = 2\left(k^2G\right)^{0.585} - 3; (k = G/B) \tag{15}$$

The Vickers hardness values for these materials are also reduced in the sequence given above. This means that the tetragonal structure, i.e., at the composition $x = 0.50$, has the lowest hardness, while the cubic structure with composition $x = 0.75$ has the highest hardness.

Table 4
The calculated bulk modulus (B), shear modulus (G), ratio of B/G, Young's modulus (E), Poisson's ratio (ν), Shear anisotropic factor (A), and Vickers hardness (H_v) of $Co_2MnGe_{1-x}Si_x$ ($x = 0$, 0.25, 0.50, 0.75, and 1) compounds for various compositions.

$Co_2MnGe_{1-x}Si_x$	Ref.	B (GPa)	G (GPa)	B/G	E (GPa)	ν	A	$\boldsymbol{H_v}$ (GPa)
$x = 0.00$	Present	187.83	96.41	1.95	246.97	0.281	2.15	10.27
	[18]	191.4	–	–	–	–	–	–
	[20]	192.70	107.5	2.68	200	0.34	1.93	–
	[23]^{GGA}	188	–	–	–	–	–	–
	[23]^{LSDA}	241	–	–	–	–	–	–
	[24]	197.6	96.4	2.05	248.7	0.29	2.44	9.5
$x = 0.25$	Present	193.87	101.17	1.92	258.53	0.278	2.05	10.91
$x = 0.50$	Present	207.27	90.29	2.30	236.53	0.309	0.79	7.54
$x = 0.75$	Present	204.35	110.30	1.85	280.44	0.271	1.87	12.23
$x = 1.00$	Present	221.02	107.34	2.06	277.15	0.291	2.05	10.24
	[18]	212.8	–	–	–	–	–	–
	[23]^{GGA}	226	–	–	–	–	–	–
	[23]^{LSDA}	264	–	–	–	–	–	–
	[24]	219.6	112.3	1.96	287.9	0.28	2.30	11.4
	[26]	227	–	–	–	–	–	–
	[27]	242.26	79.54	3.04	215.08	0.35	1.83	–
	[28]	221	71	–	–	–	–	–

Table 5
The calculated density (ρ in g.cm^{-3}), the longitudinal, transverse and average sound velocity (V_l, V_t, and V_m in m.s^{-1}), the Debye temperature (θ_D) and the melting temperature (T_{melt}) of $Co_2MnGe_{1-x}Si_x$ ($x = 0$, 0.25, 0.50, 0.75, and 1) compounds.

$Co_2MnGe_{1-x}Si_x$	Ref.	ρ(g/cm^3)	$\boldsymbol{V_l}$ (m/s)	$\boldsymbol{V_t}$(m/s)	$\boldsymbol{V_m}$(m/s)	θ_D (K)	$\boldsymbol{T_{melt}}$(K)
$x = 0.00$	Present	8.678	6038	3333	3714	486.49	2144 ± 300
	[20]	–	6309	3523	4238	–	–
	[24]	8.665	6135	3335	3720	487	2165
	[29]	–	–	–	–	549.1	–
$x = 0.25$	Present	8.398	6257	3471	3866	508.71	2217 ± 300
$x = 0.50$	Present	8.095	6362	3340	3735	493.44	2671 ± 300
$x = 0.75$	Present	7.816	6705	3757	4181	555.33	2359 ± 300
$x = 1.00$	Present	7.509	6964	3781	4218	562.85	2410 ± 300
	[24]	7.424	7054	3890	4335	576	2388
	[29]	–	–	–	–	611.4	–

Table 6
The calculated total and atomic magnetic moments of $Co_2MnGe_{1-x}Si_x$ ($x = 0$, 0.25, 0.50, 0.75, and 1) compounds for various compositions.

Composition	Ref.	M_t (μ_B)	M_{Co} (μ_B)	$M_{Mn(1)}$ (μ_B)	$M_{Mn(2)}$ (μ_B)	M_{Ge} (μ_B)	M_{Si} (μ_B)
Co_2MnGe	Present	5.00	1.01	3.01	–	−0.05	–
	[16]$^{Exp.}$	5.11	0.75	3.61	–	–	–
	[22]$^{Exp.}$	4.93	–	–	–	–	–
	[18]	5.01	–	–	–	–	–
	[20]	4.99	1.02	3.05	–	−0.05	–
	[22]	5.00	1.02	3.06	–	–	–
	[23]^{LSDA}	5.00	1.02	2.88	–	−0.02	–
	[23]^{GGA}	5.00	1.02	2.98	–	−0.03	–
	[25]	5.00	0.97	3.09	–	−0.04	–
$Co_2MnGe_{0.75}Si_{0.25}$	Present	5.00	1.02	3.11	2.95	−0.04	−0.05
$Co_2MnGe_{0.5}Si_{0.5}$	Present	5.00	1.03	3.05	2.90	−0.04	−0.05
$Co_2MnGe_{0.25}Si_{0.75}$	Present	5.00	1.04	2.84	2.99	−0.04	−0.05
Co_2MnSi	Present	5.00	1.05	2.93	–	–	−0.04
	[16]$^{Exp.}$	5.07	0.75	3.57	–	–	–
	[22]$^{Exp.}$	4.90	–	–	–	–	–
	[18]	5.00	–	–	–	–	–
	[19]	5.00	0.98	3.13	–	–	−0.09
	[22]	5.00	1.00	3.00	–	–	–
	[23]^{LSDA}	5.00	1.07	2.81	–	–	−0.02
	[23]^{GGA}	5.00	1.06	2.92	–	–	−0.04
	[26]	5.00	1.07	2.87	–	–	−0.04
	[27]	5.02	1.05	2.94	–	–	−0.04
	[28]	5.00	1.02	2.99	–	–	–

IV. The ratio between bulk modulus and shear modulus, i.e., B/G gives the ductile and brittle nature of a material. If the value of B/G is greater or less than 1.75 then the material is ductile or brittle, respectively [58]. It is seen from Table 4 for $Co_2MnGe_{1-x}Si_x$ compounds that the values of the ratio B/G are greater than the critical value, which is 1.75. This result indicates that the $Co_2MnGe_{1-x}Si_x$ compounds are ductile in nature.

V. The Poisson's ratios (ν) of the studied compounds have been calculated using obtained B and G with the help of the relationship given in Eq. (16) and the results are presented in Table 4. The

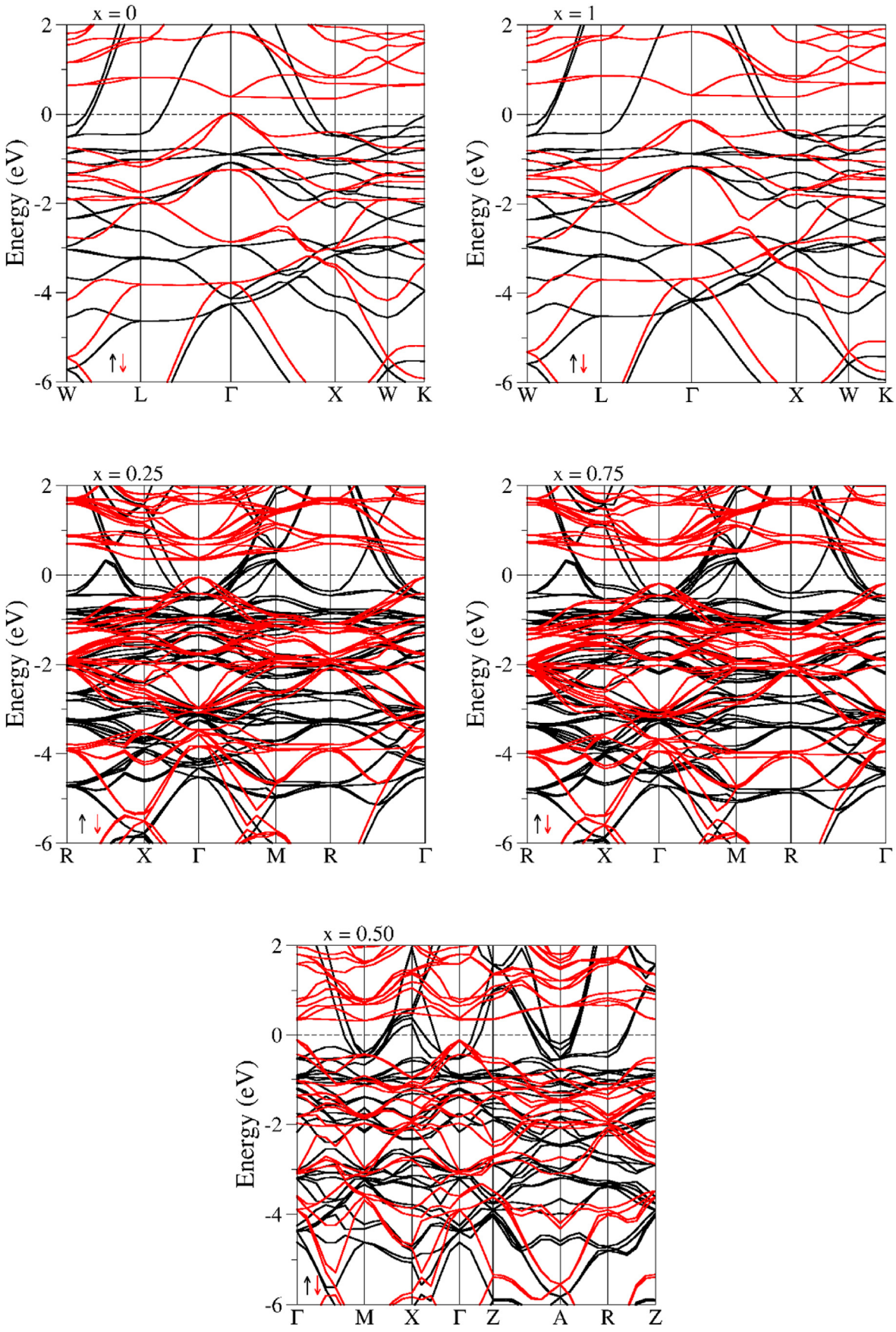

Fig. 2. Spin-polarized band structures of $Co_2MnGe_{1-x}Si_x$ (x = 0, 0.25, 0.5, 0.75, and 1) compounds. (For interpretation of the references to colour in this figure legend, the reader is referred to the Web version of this article.)

Table 7
E_{min} and E_{max} are the values of the minimum energy of the conduction band and the maximum energy of the valence band, bandgap (E_g), half-metallic bandgap (E_{HM}) and density of states at Fermi energy [$N\uparrow$ (E_F), $N\downarrow$ (E_F)] for $Co_2MnGe_{1-x}Si_x$ ($x = 0$, 0.25, 0.50, 0.75, and 1) compounds.

Composition	Ref.	E_{min} (eV)	E_{max} (eV)	E_g (eV)	E_{HM} (eV)	$N\uparrow$ (E_F)	$N\downarrow$ (E_F)
Co_2MnGe	Present	0.350	−0.014	0.36	0.014	1.31	0
	[18]	–	–	0.59	–	1.33	0
	[20]	0.48	−0.010	0.49	0.010	1.38	0
	[21]	–	–	0.21	–	–	–
	[22]	0.533	−0.048	0.581	0.048	1.29	–
	[23]	–	–	0.54	–	–	–
	[25]	–	–	0.60	–	–	–
	[29]	–	–	0.34	–	–	–
$Co_2MnGe_{0.75}Si_{0.25}$	Present	0.335	−0.047	0.38	0.047	5.23	0
$Co_2MnGe_{0.5}Si_{0.5}$	Present	0.321	−0.118	0.44	0.118	2.24	0
$Co_2MnGe_{0.25}Si_{0.75}$	Present	0.341	−0.191	0.53	0.191	5.74	0
Co_2MnSi	Present	0.316	−0.259	0.57	0.259	1.14	0
	[18]	–	–	0.77	–	1.17	0
	[21]	–	–	0.419	–	–	–
	[22]	0.506	−0.292	0.798	0.292	1.27	–
	[23]	–	–	0.81	–	–	–
	[26]	–	–	0.82	–	–	–
	[28]	–	–	0.66	–	0.31	0
	[29]	–	–	0.55	–	–	–

Poisson's ratio is used to determine the covalent or ionic character of the materials, and this value is 0.25 for ionic materials and it is 0.1 for covalent materials. Since the Poisson's ratio of the $Co_2MnGe_{1-x}Si_x$ ($x = 0$, 0.25, 0.50, 0.75, and 1) compounds is between 0.271 and 0.309, these compounds have ionic character.

$$v = \frac{1}{2}\left[\frac{B - \frac{2}{3}G}{B + \frac{1}{3}G}\right] \tag{16}$$

VI. The elastic anisotropy of any material represents that the micro-cracks can be easily created in the material. For a cubic [59] and tetragonal [60] structure, the anisotropy factor can be given in terms of elastic constants as follows, respectively. Besides, the results are given in Table 4:

$$A = \frac{2C_{44}}{(C_{11} - C_{12})} \text{for cubic,} \tag{17}$$

$$A = \frac{C_{44}\,(C_{11} + 2C_{13} + C_{33})}{\left(C_{11}C_{33} - C_{13}^2\right)} \text{for tetragonal} \tag{18}$$

It is also known that if $A = 1$ then the materials are isotropic in nature and deviation from this value represents that the material is anisotropic in nature. Table 4 shows that the studied compounds are anisotropic because the calculated A values of $Co_2MnGe_{1-x}Si_x$ for all compositions of x are not 1.

The Debye temperature (θ_D) is an important property for any solid which correlates the specific heat and the melting temperature of the corresponding solid. θ_D is calculated from the following equation by using the obtained bulk and shear modulus [61].

$$\theta_D = \frac{h}{k_B}\left[\frac{3n}{4\pi}\frac{N_A\rho}{M}\right]^{1/3}.V_m \tag{19}$$

where h, k_B, n, N_A, ρ, and M are the Plank's constant, Boltzmann's constant, number of atoms in the molecule, Avogadro's number, mass density, and molecular weight, respectively. The average elastic wave velocity V_m for the $Co_2MnGe_{1-x}Si_x$ ($x = 0$, 0.25, 0.50, 0.75, and 1) can be calculated by the following relation [62]:

$$V_m = \left[\frac{1}{3}\left(\frac{2}{v_t^3} + \frac{1}{v_l^3}\right)\right]^{-1/3} \tag{20}$$

where, V_l is the transverse elastic wave velocity and V_t is the longitudinal elastic wave velocity and they can be calculated with the following relations [63]:

$$V_l = \sqrt{\frac{3B + 4G}{3\rho}};\; V_t = \sqrt{\frac{G}{\rho}} \tag{21}$$

The calculated density (ρ), transverse (V_l), longitudinal (V_t), average (V_m) velocities and Debye temperatures (θ_D) for the $Co_2MnGe_{1-x}Si_x$ ($x = 0$, 0.25, 0.50, 0.75, and 1) compounds have been tabulated in Table 5. The obtained Debye temperatures decrease in the sequence of $Co_2MnSi > Co_2MnGe_{0.25}Si_{0.75} > Co_2MnGe_{0.75}Si_{0.25} > Co_2MnGe_{0.50}Si_{0.50} > Co_2MnGe$.

Additionally, the melting temperatures (T_{melt}) are calculated using the following relation [64],

$$T_{melt} = \left[553 + \left(\frac{5.91C_{11}}{GPa}\right)\right]K \mp 300K \tag{22}$$

and the obtained results for $Co_2MnGe_{1-x}Si_x$ ($x = 0$, 0.25, 0.50, 0.75, and 1) compounds are given in Table 5. It is found that the $Co_2MnGe_{0.50}Si_{0.50}$ compound with tetragonal structure has the highest melting temperature.

3.3. Magnetic properties and slater pauling behavior

The calculated atomic and total magnetic moments for the studied compounds $Co_2MnGe_{1-x}Si_x$ at various compositions of x ($x = 0$, 0.25, 0.50, 0.75, and 1) are given in Table 6. The total magnetic moment for Co_2MnGe ($x = 0$) is mainly due to the magnetic moments of the Mn and Co atoms and the contribution of Ge atoms to magnetic moment is very small. The magnetic properties of any compound basically depend on the constituent atoms and the position of atoms with respect to the origin of atoms. Hence the magnetic moments of any compounds depend on the structure of the compounds. However, Si and Ge are 4A group elements, the number of valence electrons in the unit cell does not change with increasing Si concentration. It is seen from Table 6 that the total

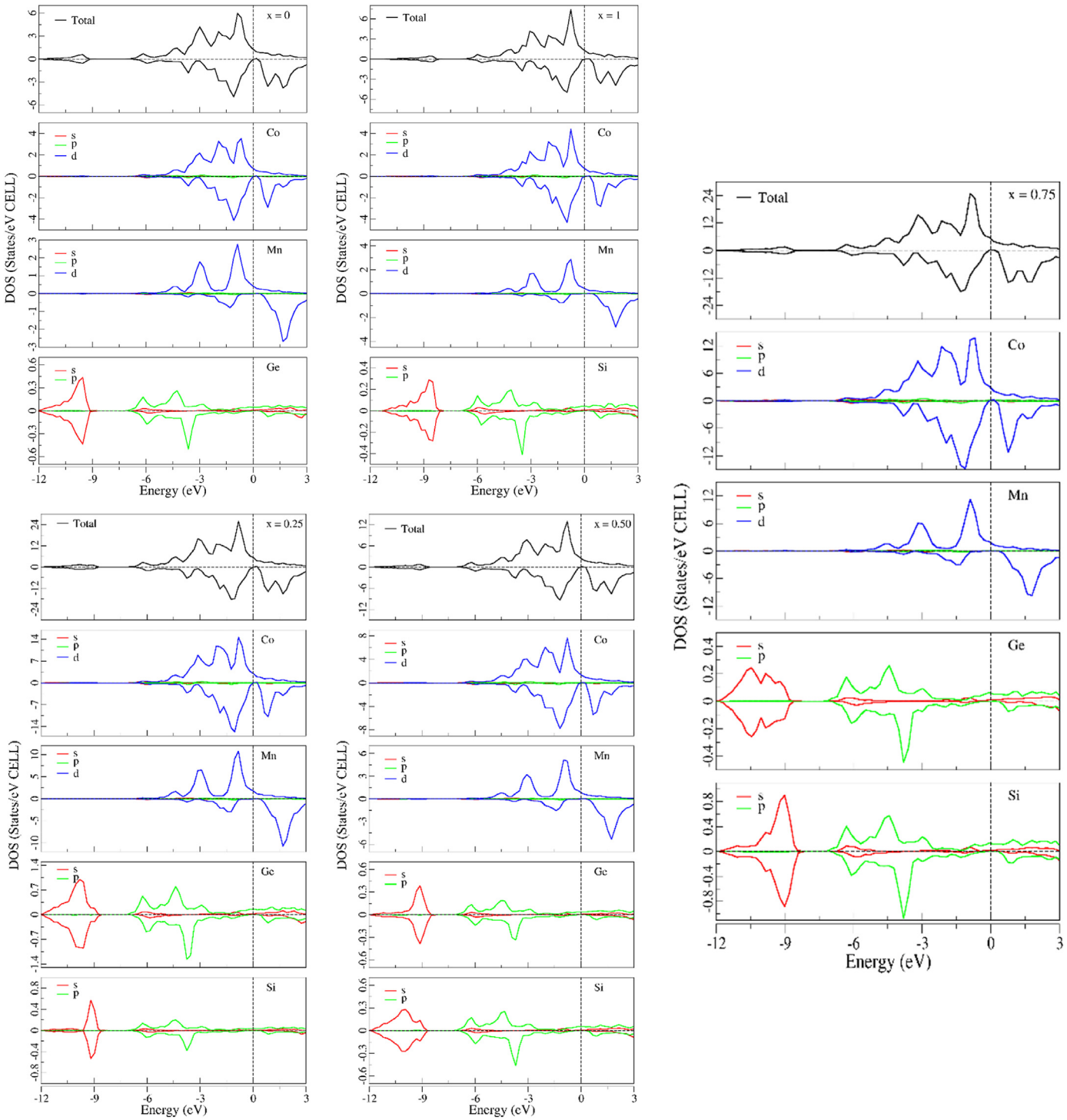

Fig. 3. Spin-polarized total and partial density of states (DOS) of $Co_2MnGe_{1-x}Si_x$ ($x = 0$, 0.25, 0.5, 0.75, and 1) compounds. (For interpretation of the references to colour in this figure legend, the reader is referred to the Web version of this article.)

magnetic moment per cell remains constant with growing Si concentration in Heusler alloys having values 5.00 μ_B, 20 μ_B/16 atoms, 20 μ_B/16 atoms, 20 μ_B/16 atoms and 5.00 μ_B for $Co_2MnGe_{1-x}Si_x$ ($x = 0$, 0.25, 0.50, 0.75, and 1), respectively.

The total magnetic moment of 3d elements and their alloys can be predicted from their average valence electron numbers N_v according to the Slater-Pauling rule. The total magnetic moment in multiples of Bohr magnetons μ_B is given by,

$$M_t = N_v - 2n_\downarrow \tag{23}$$

where N_v is the average number of valence electrons per atom and $2n_\downarrow$ is the number of minority state electrons. The minimum in the minority density of states forces the number of electrons in the d minority band to be nearly three. Ignoring the s and p electrons, the total magnetic moment per atom can be calculated as,

$$M_t = N_v - 6 \quad (24)$$

In the case of full Heusler compounds, there are four atoms per unit cell leading to the formula,

$$M_t = N_v - 24 \quad (25)$$

The stoichiometric Co_2MnGe and Co_2MnSi full Heusler compounds have 29 valence electrons. According to Eq. (25), the estimated total magnetic moment is 5 μ_B for both compounds. The calculated integral values of the total magnetic moment for the stoichiometric Co_2MnGe and Co_2MnSi alloys give the expected result for half-metallic ferromagnet compounds accordingly Slater–Pauling behavior. In the event of non-stoichiometric $Co_2MnGe_{0.75}Si_{0.25}$, $Co_2MnGe_{0.50}Si_{0.50}$, and $Co_2MnGe_{0.25}Si_{0.75}$ compounds, the partial substitution of the Ge atom by the Si one does not affect the atomic magnetic moment or the total magnetic moment (see Table 6). Ge and Si belong to the same column of the periodic table, so the substitution of Ge by Si does not change the number of valence electrons. Therefore, the total and atomic magnetic moments will remain the same.

3.4. Electronic properties

According to the spin-up and spin-down states, electronic band structures along the high symmetry directions of $Co_2MnGe_{1-x}Si_x$ ($x = 0$, 0.25, 0.50, 0.75, and 1) Heusler compounds are plotted using the first-principles methods and these are shown in Fig. 2. As sketched in Fig. 2, all compounds have a direct bandgap and the Fermi level is also situated within this bandgap. As for the spin-up state, the valence and conduction bands are overlapping, and the Fermi level is cutting them. This indicates that non-stoichiometric $Co_2MnGe_{1-x}Si_x$ (x = 0.25, 0.50, 0.75) as well as Co_2MnSi and Co_2MnGe pure compounds are half-metallic materials.

In an attempt to the better investigation of the electronic characteristic of these five compounds, two parameters have been presented, which are bandgap and half-metallic bandgap [65–68]. The bandgap is the sum of the valence band maximum (E_{max}) and conduction band minimum (E_{min}). On the other hand, the half-metallic bandgap can be known as the minimum absolute value between E_{max} and E_{min}. The conduction band minimum (E_{min}) and the valence band maximum (E_{max}), bandgap and the half-metallic bandgap of $Co_2MnGe_{1-x}Si_x$ (x = 0, 0.25, 0.50, 0.75, and 1) Heusler compounds have been given in Table 7. The calculated band gaps for the $Co_2MnGe_{1-x}Si_x$ (x = 0, 0.25, 0.50, 0.75, and 1) compounds are 0.36 eV, 0.38 eV, 0.44 eV, 0.53 eV and 0.57 eV, respectively. In addition, the estimated half-metallic band gaps of $Co_2MnGe_{1-x}Si_x$ (x = 0, 0.25, 0.50, 0.75 and 1) compounds are 0.014, 0.047, 0.118, 0.191 and 0.259, respectively. The band and half-metallic band gaps of $Co_2MnGe_{1-x}Si_x$ ($x = 0$, 0.25, 0.50, 0.75 and 1) with the growing Si constituent slightly increase. Additionally, the obtained band gap (E_g) and half-metallic bandgap (E_{HM}) values for Co_2MnSi and Co_2MnGe agree well with previous studies [18,20–23,25,26,28,29]. As a result, all compounds are ideal candidates for applications in spin-electronics devices.

We also calculated the spin-polarized total and partial density of states of the studied materials at various compositions of x and plotted them in Fig. 3. From the density of states relation given in Fig. 3, we can make the following explanations for different compositions of x ($x = 0.25$, 0.50, 0.75, and 1). When $x = 0.25$, the main contribution to the density of states (DOS) for Co and Mn comes from d orbitals. However, for the Ge atom between −12 eV and −9 eV, the main contribution arises from s orbitals and also between −6 eV and +3 eV the main contribution arises from p orbitals. For x = 0.5, the main contribution to DOS stems from d orbitals for Co and Mn. Between −12 eV and −9 eV for Ge and Si, most of the contribution come from s orbitals, while most of the contribution that are coming from p orbitals between −6 eV and +3 eV. When $x = 0.75$, the contribution of orbitals for Co, Mn, Ge, and Si is the same as $x = 0.5$ as mentioned above. For the case of $x = 1$, the majority of the contribution to DOS for Co and Mn results from d orbitals. And for Si between −11 eV and −8 eV majority of the contribution consists of s orbitals and between −7 eV and +3 eV majority of the contribution consists of p orbitals.

4. Conclusions

The effects of Si composition on the structural, magnetic, electronic, and mechanical properties of the $Co_2MnGe_{1-x}Si_x$ (x = 0, 0.25, 0.50, 0.75, and 1) compounds are investigated by the ab initio calculations within density functional theory (DFT). The structural parameters acquired through the GGA-PBE are in harmony with the experimental and theoretical values presented in the literature. It is detected that the calculated lattice constants and enthalpy of formation for $Co_2MnGe_{1-x}Si_x$ compounds decrease with increasing Si substitution. Thus, these compounds have become more thermodynamically stable with increasing concentration x. The calculated band gap values of the $Co_2MnGe_{1-x}Si_x$ (x = 0, 0.25, 0.50, 0.75, and 1) compounds are 0.36 eV, 0.38 eV, 0.44 eV, 0.53 eV and 0.57 eV, respectively. These compounds have shown half-metallic character. Therefore, they are ideal candidates for applications in spintronics and magnetoelectronics areas. In addition, the bandgap and half-metallic band gap increase with the growing Si constituent. Moreover, the computed total magnetic moments for these compounds comply with the Slater–Pauling rule. It is estimated that they are mechanically stable at all compositions of x because these compounds satisfy Born's stability criterion. Moreover, the compounds $Co_2MnGe_{1-x}Si_x$ have ductility behavior at all compositions of x. Besides, the cubic structure with composition x = 0.75 has the highest hardness while the tetragonal structure with composition $x = 0.5$ has the lowest hardness. These materials with half-metallic ferromagnet property could be a significant nominee for spintronic devices and could also be used in certain technological applications due to their ductility behavior.

CRediT authorship contribution statement

M. Özduran: Investigation, Methodology. **A. Candan:** Conceptualization, Methodology, Software, Writing - review & editing. **S. Akbudak:** Investigation, Writing - original draft, Writing - review & editing. **A.K. Kushwaha:** Investigation, Writing - original draft. **A. İyigör:** Formal analysis, Data curation.

Declaration of competing interest

The authors declare that they have no known competing financial interests or personal relationships that could have appeared to influence the work reported in this paper.

References

[1] F. Heusler, Verhandlungen Dtsch. Phys. Ges. 5 (1903) 219.
[2] T.M. Bhat, D.C. Gupta, Magneto-electronic, thermal, and thermoelectric properties of some Co-based quaternary alloys, J. Phys. Chem. Solid. 112 (2018) 190–199.
[3] S.A. Khandy, I. Islam, D.C. Gupta, R. Khenata, A. Laref, Lattice dynamics, mechanical stability and electronic structure of Fe-based Heusler semiconductors, Sci. Rep. 9 (2019) 1475.
[4] L. Bainsla, K.G. Suresh, Equiatomic quaternary Heusler alloys: a material perspective for spintronic applications, Appl. Phys. Rev. 3 (2016), 031101.
[5] F. Casper, T. Graf, S. Chadov, B. Balke, C. Felser, Half-Heusler compounds: novel materials for energy and spintronic applications, Semicond. Sci. Technol. 27 (2012), 063001.
[6] A. Amudhavalli, R. Rajeswarapalanichamy, K. Iyakutti, A.K. Kushwaha, First

principles study of structural and optoelectronic properties of Li based half Heusler alloys, Comp. Cond. Matt. 14 (2018) 55–66.
[7] S. Kacimi, H. Mehnane, A. Zaoui, I–II–V and I–III–IV half-Heusler compounds for optoelectronic applications: comparative ab initio study, J. Alloys Compd. 587 (2014) 451–458.
[8] L. Bainsla, A.I. Mallick, M.M. Raja, A.K. Nigam, B.S.D. Ch S. Varaprasad, Y.K. Takahashi, A. Alam, K.G. Suresh, K. Hono, Spin gapless semiconducting behavior in equiatomic quaternary CoFeMnSi Heusler alloy, Phys. Rev. B 91 (2015) 104408.
[9] A. Planes, L. Mañosa, M. Acet, Magnetocaloric effect and its relation to shape-memory properties in ferromagnetic Heusler alloys, J. Phys. Condens. Matter 21 (2009) 233201.
[10] T.M. Tritt, M.A. Subramanian, Thermoelectric materials, phenomena, and applications: a bird's eye view, MRS Bull. 31 (2006) 188–198.
[11] M.N. Baibich, J.M. Broto, A. Fert, F. Nguyen Van Dau, F. Petroff, P. Etienne, G. Creuzet, A. Friederich, J. Chazelas, Giant magnetoresistance of (001) Fe/(001)Cr magnetic superlattices, Phys. Rev. Lett. 61 (1988) 2472.
[12] G. Binasch, P. Grünberg, F. Saurenbach, W. Zinn, Enhanced magnetoresistance in layered magnetic structures with antiferromagnetic interlayer exchange, Phys. Rev. B 39 (1989) 4828.
[13] R.A. De Groot, F.M. Mueller, P.G. Van Engen, K.H.J. Buschow, New class of materials: half-metallic ferromagnets, Phys. Rev. Lett. 50 (1983) 2024.
[14] J.H. Wernick, G.W. Hull, T.H. Geballe, J.E. Bernardini, J.V. Waszczak, Superconductivity in ternary Heusler intermetallic compounds, Mater. Lett. 2 (1983) 90–92.
[15] K. Watanabe, On new ferromagnetic intermetallic compounds PtMnSn and PtMnSb, J. Phys. Soc. Jpn. 28 (1970) 302–307.
[16] P.J. Webster, Magnetic and chemical order in Heusler alloys containing cobalt and manganese, J. Phys. Chem. Solid. 32 (1971) 1221–1231.
[17] A.S. Manea, O. Monnereau, R. Notonier, F. Guinneton, C. Logofatu, L. Tortet, A. Garnier, M. Mitrea, C. Negrila, W. Branford, C.E.A. Grigorescu, Heusler bulk materials as targets for pulsed laser deposition: growth and characterization, J. Cryst. Growth 275 (2005) e1787–e1792.
[18] A. Candan, G. Uğur, Z. Charifi, H. Baaziz, M.R. Ellialtıoğlu, Electronic structure and vibrational properties in cobalt-based full-Heusler compounds: a first principle study of Co_2MnX (X= Si, Ge, Al, Ga), J. Alloys Compd. 560 (2013) 215–222.
[19] I. Galanakis, K. Özdogan, E. Şaşioğlu, Role of defects and disorder in the half-metallic full-Heusler compounds, in: Advances in Nanoscale Magnetism, Springer, Berlin, Heidelberg, 2009, pp. 1–19.
[20] A. Akriche, B. Abidri, S. Hiadsi, H. Bouafia, B. Sahli, Half-metallic properties and the robustness of Co_2MnGe Heusler alloy under pressure: ab-initio calculation, Intermetallics 68 (2016) 42–50.
[21] S. Ishida, S. Fujii, S. Kashiwagi, S. Asano, Search for half-metallic compounds in Co_2MnZ (Z= IIIb, IVb, Vb element), J. Phys. Soc. Jpn. 64 (1995) 2152–2157.
[22] H.C. Kandpal, G.H. Fecher, C. Felser, Calculated electronic and magnetic properties of the half-metallic, transition metal based Heusler compounds, J. Phys. D Appl. Phys. 40 (2007) 1507.
[23] S. Picozzi, A. Continenza, A.J. Freeman, Co_2MnX (X= Si, Ge, Sn) Heusler compounds: an ab initio study of their structural, electronic, and magnetic properties at zero and elevated pressure, Phys. Rev. B 66 (2002), 094421.
[24] S.C. Wu, G.H. Fecher, S. Shahab Naghavi, C. Felser, Elastic properties and stability of Heusler compounds: cubic Co_2YZ compounds with $L2_1$ structure, J. Appl. Phys. 125 (2019), 082523.
[25] D.P. Rai, M.P. Ghimire, R.K. Thapa, Ground state study of electronic and magnetic properties of Co_2MnZ (Z= Ge, Sn) type Heusler compounds: a first principle study, J. Phys.: Conf. Ser. 377 (2012), 012074.
[26] H. Ido, Induced magnetic moment on Co below TC in the ferromagnetic Heusler-type alloys Co_2MnX (X= Si, Ge and Sn), J. Magn. Magn Mater. 54 (1986) 937–938.
[27] S. Amari, R. Mebsout, S. Méçabih, B. Abbar, B. Bouhafs, First-principle study of magnetic, elastic and thermal properties of full Heusler Co_2MnSi, Intermetallics 44 (2014) 26–30.
[28] X.Q. Chen, R. Podloucky, P. Rogl, Ab initio prediction of half-metallic properties for the ferromagnetic Heusler alloys Co_2MSi (M= Ti, V, Cr), J. Appl. Phys. 100 (2006) 113901.
[29] M.A. Zagrebin, V.V. Sokolovskiy, V.D. Buchelnikov, Electronic and magnetic properties of the Co_2-based Heusler compounds under pressure: first-principles and Monte Carlo studies, J. Phys. D Appl. Phys. 49 (2016) 355004.
[30] M. Yin, S. Chen, P. Nash, Enthalpies of formation of selected Co_2YZ Heusler compounds, J. Alloys Compd. 577 (2013) 49–56.
[31] B.A. Alhaj, B. Hamad, Ab-initio calculations of the electronic and magnetic structures of $Co_2Cr_{1-x}Mn_xAl$ alloys, J. Appl. Phys. 112 (2012) 123904.
[32] B.A. Alhaj, B. Hamad, J. Khalifeh, R. Shaltaf, Ab-initio calculations of the electronic and magnetic structures of $Co_2Cr1\text{-}_xMn_xSi$ alloys, J. Magn. Magn Mater. 336 (2013) 37–43.
[33] Q.F. Li, J.G. Yin, X.F. Zhu, Theoretical study of the electronic and magnetic properties of $Co_2Cr_{1-x}V_xAl$, J. Magn. Magn Mater. 322 (2010) 2293–2297.
[34] M. Guezlane, H. Baaziz, F.E.H. Hassan, Z. Charifi, Y. Djaballah, Electronic, magnetic and thermal properties of $Co_2Cr_xFe_{1-x}X$ (X= Al, Si) Heusler alloys: first-principles calculations, J. Magn. Magn Mater. 414 (2016) 219–226.
[35] G. Kresse, J. Furthmüller, Efficiency of ab-initio total energy calculations for metals and semiconductors using a plane-wave basis set, Comput. Mater. Sci. 6 (1996) 15–50.
[36] G. Kresse, J. Furthmüller, Efficient iterative schemes for ab initio total-energy calculations using a plane-wave basis set, Phys. Rev. B 54 (1996) 11169.
[37] P.E. Blöchl, Projector augmented-wave method, Phys. Rev. B 50 (1994) 17953.
[38] G. Kresse, D. Joubert, From ultrasoft pseudopotentials to the projector augmented-wave method, Phys. Rev. B 59 (1999) 1758.
[39] J.P. Perdew, K. Burke, M. Ernzerhof, Generalized gradient approximation made simple, Phys. Rev. Lett. 77 (1996) 3865.
[40] M. Methfessel, A.T. Paxton, High-precision sampling for Brillouin-zone integration in metals, Phys. Rev. B 40 (1989) 3616.
[41] H.J. Monkhorst, J.D. Pack, Special points for Brillouin-zone integrations, Phys. Rev. B 13 (1976) 5188.
[42] O.H. Nielsen, R.M. Martin, First-principles calculation of stress, Phys. Rev. Lett. 50 (1983) 697.
[43] A. Candan, S. Akbudak, M. Özduran, A. İyigör, An examination of the structural, electronic, elastic, vibrational and thermodynamic properties of Ru_2YGa (Y= Sc, Ti and V) Heusler alloys, Chin. J. Phys. 56 (2018) 1772–1780.
[44] S. Noui, Z. Charifi, H. Baaziz, G. Uğur, Ş. Uğur, Effect of structure on the electronic, magnetic and thermal properties of cubic $Fe_2Mn_xNi_{1-x}Si$ Heusler alloys, J. Electron. Mater. 48 (2019) 337–351.
[45] F. Semari, F. Dahmane, N. Baki, Y. Al-Douri, S. Akbudak, G. Uğur, Ş. Uğur, A. Bouhemadou, R. Khenata, C.H. Voon, First-principle calculations of structural, electronic and magnetic investigations of $Mn_2RuGe_{1-x}Sn_x$ quaternary Heusler alloys, Chin. J. Phys. 56 (2018) 567–573.
[46] M.P. Raphael, B. Ravel, M.A. Willard, S.F. Cheng, B.N. Das, R.M. Stroud, K.M. Bussmann, J.H. Claassen, V.G. Harris, Magnetic, structural, and transport properties of thin film and single crystal Co_2MnSi, Appl. Phys. Lett. 79 (2001) 4396–4398.
[47] S.J. Ahmed, C. Boyer, M. Niewczas, Magnetic and structural properties of Co_2MnSi based Heusler compound, J. Alloys Compd. 781 (2019) 216–225.
[48] T. Lantri, S. Bentata, B. Bouadjemi, W. Benstaali, B. Bouhafs, A. Abbad, A. Zitouni, Effect of Coulomb interactions and Hartree-Fock exchange on structural, elastic, optoelectronic and magnetic properties of Co_2MnSi Heusler: a comparative study, J. Magn. Magn Mater. 419 (2016) 74–83.
[49] F. Dahmane, B. Doumi, Y. Mogulkoc, A. Tadjer, D. Prakash, K.D. Verma, D. Varshney, M.A. Ghebouli, S. Bin Omran, R. Khenata, Investigations of the structural, electronic, magnetic, and half-metallic behavior of Co_2MnZ (Z= Al, Ge, Si, Ga) Full-Heusler compounds, J. Supercond. Nov. Magnetism 29 (2016) 809–817.
[50] L. Vegard, Formation of mixed crystals by solid-phase contact, J. Phys. 5 (1921) 393–395.
[51] A.K. Kushwaha, C.G. Ma, M.G. Brik, S. Bin Omran, R. Khenata, Zone-center phonons and elastic properties of ternary chalcopyrite $ABSe_2$ (A= Cu and Ag; B= al, Ga and In), Mater. Chem. Phys. 227 (2019) 324–331.
[52] X. Gao, Y. Jiang, R. Zhou, J. Feng, Stability and elastic properties of Y–C binary compounds investigated by first principles calculations, J. Alloys Compd. 587 (2014) 819–826.
[53] B. Huang, Y.H. Duan, Y. Sun, M.J. Peng, S. Chen, Electronic structures, mechanical and thermodynamic properties of cubic alkaline-earth hexaborides from first principles calculations, J. Alloys Compd. 635 (2015) 213–224.
[54] W. Voigt, Lehrbuch der Kristallphysik, Teubner, Leipzig, 1928.
[55] A. Reuss, Account of the liquid limit of mixed crystals on the basis of the plasticity condition for single crystal, Z. Angew. Math. Mech. 9 (1929) 49–58.
[56] R. Hill, The elastic behaviour of a crystalline aggregate, Proc. Phys. Soc. 65 (1952) 349.
[57] A. Candan, S. Akbudak, Ş. Uğur, G. Uğur, Theoretical research on structural, electronic, mechanical, lattice dynamical and thermodynamic properties of layered ternary nitrides Ti_2AN (A= Si, Ge and Sn), J. Alloys Compd. 771 (2019) 664–673.
[58] S.F. Pugh, XCII. Relations between the elastic moduli and the plastic properties of polycrystalline pure metals, Lond. Edinburgh Dublin Philos. Mag. J. Sci. 45 (1954) 823–843.
[59] S.I. Ranganathan, M. Ostoja-Starzewski, Universal elastic anisotropy index, Phys. Rev. Lett. 101 (2008), 055504.
[60] F. Parvin, S.H. Naqib, Structural, elastic, electronic, thermodynamic, and optical properties of layered $BaPd_2As_2$ pnictide superconductor: a first principles investigation, J. Alloys Compd. 780 (2019) 452–460.
[61] P. Wachter, M. Filzmoser, J. Rebizant, Phys. B Condens. Matter 293 (2001) 199–223.
[62] O.L. Anderson, A simplified method for calculating the Debye temperature from elastic constants, J. Phys. Chem. Solid. 24 (1963) 909–917.
[63] E. Schreiber, O.L. Anderson, N. Soga, J.F. Bell, Elastic constants and their measurement, J. Appl. Mech. 42 (1975) 747–748.
[64] M.E. Fine, L.D. Brown, H.L. Marcus, Elastic constants versus melting temperature in metals, Scripta Metall. 18 (1984) 951–956.
[65] Y. Han, X. Wang, First-principles investigation of half-metallic ferromagnetism of a new 1: 1: 1: 1 type quaternary heusler compound YRhTiSi, J. Supercond. Nov. Magnetism 32 (6) (2019) 1681–1689.
[66] W. Liu, X. Zhang, H. Jia, R. Khenata, X. Dai, G. Liu, Theoretical investigations on the mechanical, magneto-electronic properties and half-metallic characteristics of ZrRhTiZ (Z= Al, Ga) quaternary heusler compounds, Appl. Sci. 9 (2019) 883.
[67] A. Erkişi, B. Yildiz, K. Demir, G. Surucu, First principles study on new half-metallic ferromagnetic ternary zinc-based sulfide and telluride (Zn_3VS_4 and Zn_3VTe_4), Mater. Res. Express 6 (2019), 076107.
[68] A. Erkisi, G. Surucu, The electronic and elasticity properties of new half-metallic chalcogenides Cu_3TMCh_4 (TM= Cr, Fe and Ch= S, Se, Te): an ab initio study, Philos. Mag. A 99 (2019) 513–529.